

1 **Title: Systems analysis shows a role of cytophilic antibodies in shaping innate**
2 **tolerance to malaria**

3 **Authors:** Maximilian Julius Lautenbach^{1,2}, Victor Yman^{1,3}, Nadir Kadri^{1,2,4}, David Fernando
4 Plaza^{1,2}, Sina Angenendt^{1,2}, Klara Sondén^{1,2}, Anna Färnert^{1,2}, Christopher Sundling^{1,2*}

5
6 **Affiliations:**

7 ¹Division of Infectious Diseases, Department of Medicine Solna, and Center for Molecular
8 Medicine, Karolinska Institutet, Stockholm, Sweden.

9 ²Department of Infectious Diseases, Karolinska University Hospital, Stockholm, Sweden.

10 ³Department of Infectious Diseases, South Stockholm Hospital, Stockholm, Sweden

11 ⁴Science for Life Laboratory, Department of Medicine Solna, Karolinska Institute.

12

13 *Corresponding author. Email: christopher.sundling@ki.se (C.S.)

14

15 **One Sentence Summary:** A systems immunology analysis on natural malaria sheds light on
16 disease tolerance mechanism associated with gamma delta T cell expansion (134/150 with
17 spaces)

18

19 **Abstract:**

20 The mechanism of acquisition and maintenance of natural immunity against *Plasmodium*
21 *falciparum* malaria remains unclear. Although, clinical immunity develops over time with repeated
22 malaria episodes, disease tolerance is more rapidly acquired compared to protective immunity. It
23 remains unclear, how pre-existing immune responses impacts the mechanism responsible for
24 disease tolerance. Here, we investigated a cohort of returning travelers treated for acute
25 symptomatic *P. falciparum* malaria, either infected for the first time, or with a previous history of
26 malaria. Through repeated sampling over one year in a malaria free setting, we were able to study
27 the acute and longitudinal effects of the infection. We combined comprehensive immune cell and
28 plasma protein profiling with integrated and data driven analysis, describing the immune landscape
29 from acute disease to one year after infection. We identified a strong association between pro-
30 inflammatory signatures and $\gamma\delta$ T cell expansion. The association was significantly impacted by
31 previous exposure to malaria, resulting in a dampened pro-inflammatory response, which
32 translated to reduced V δ ²⁺ $\gamma\delta$ T cell expansion compared to primary infected individuals. The
33 dampened inflammatory signal was associated with early expansion of Fc γ RIII⁺ monocytes and
34 parasite-specific antibodies of IgG1 and IgG3 isotypes.

35 Our data suggest that the interplay of Fc γ RIII⁺ monocytes and a cytophilic parasite-specific IgG
36 during the early blood stage infection lead to lower parasitemia and a dampened pro-inflammatory
37 response with reduced $\gamma\delta$ T cell expansion. This enhanced control and reduced inflammation points
38 to a potential mechanism on how tolerance is established following repeated malaria exposure.
39 (244/250 words)

40

41 **Main Text:**

42 **INTRODUCTION**

43 Malaria remains a global burden with an estimated 229 million malaria cases leading to
44 approximately 409 000 deaths in 2019 (1). Compared to other pathogens, immunity to malaria is
45 slow to develop (2). In malaria endemic areas, partial immunity is acquired over time after repeated
46 infections. Clinical symptoms are reduced while low grade subclinical infections remain and allow
47 for continued parasite transmission (2, 3). However, protection from severe forms of malaria,
48 despite high levels of parasitemia, seem to develop already after a few infections (4). A recent
49 study by Nahrendorf and colleagues suggests a tolerance mechanism where better control of host-
50 damaging factors that are part of the natural immune response to infection are an underlying cause
51 for the reduced severity (5). Currently no study has investigated how long tolerance persists and
52 how it is maintained in response to malaria.

53 Clinical symptoms are due to the blood stage of the infection, where merozoites invade
54 erythrocytes that then sequester, followed by parasite multiplication before bursting out to infect
55 new erythrocytes (6). The clinical manifestations are partly due to the strong innate pro-
56 inflammatory response, during the parasite blood stage/to the *P. falciparum* blood stage (7).

57 Much of our current understanding of the immune responses to *P. falciparum* infection is based
58 on hypothesis-driven research, where selected cell subsets, inflammatory markers, or clinical
59 features are investigated at a time (8, 9). Improved technology and bioinformatic tools enable the
60 analysis of high-dimensional parameters in limited sample material, giving us the opportunity to
61 study complex immune responses at a systems level to provide new insights into complex
62 immunological networks that represent the immune response during infection (10). Systems level
63 approaches to study febrile/non-febrile children in malaria endemic countries (11) as well as the
64 comparison of malaria naïve and Africans in controlled human malaria infection (CHMI) studies
65 (12) have generated valuable findings and new hypotheses. While studies in endemic populations
66 allow investigation of acute naturally acquired malaria and persistent (largely asymptomatic)
67 infections in the context of previous exposure. Despite CHMI studies enable more control over
68 prior parasite exposure, infectious dose, and follow-up after infection, although only in the context
69 of very low level parasitemia and often before symptoms having appeared. Although compensating
70 for some limitations, CHMI cannot fully mirror a natural infection, due to early treatment not
71 allowing observation of potential effects derived from a strong natural symptomatic infection. This

72 leaves a knowledge gap on how natural infection affects the immune response in the absence of
73 potential parasite re-exposure. This gap can be filled by investigating the immune response after
74 naturally acquired malaria in individuals leaving the endemic area, seeking healthcare in a setting
75 without risk of re-exposure.

76 Here, we study a prospective cohort of returning travelers treated for acute *P. falciparum* malaria
77 at the Karolinska University Hospital in Sweden, followed over one year after infection. Using a
78 systems immunology approach and data-driven analysis, we combined plasma protein and cell
79 profiling to study dynamic changes of the immune response over time in these patients. Based on
80 our results, we propose a model where antibody-derived memory modulates the pro-
81 inflammatory cytokine response which in turn impact $\gamma\delta$ T cell expansion and improve disease
82 tolerance.

83

84 RESULTS

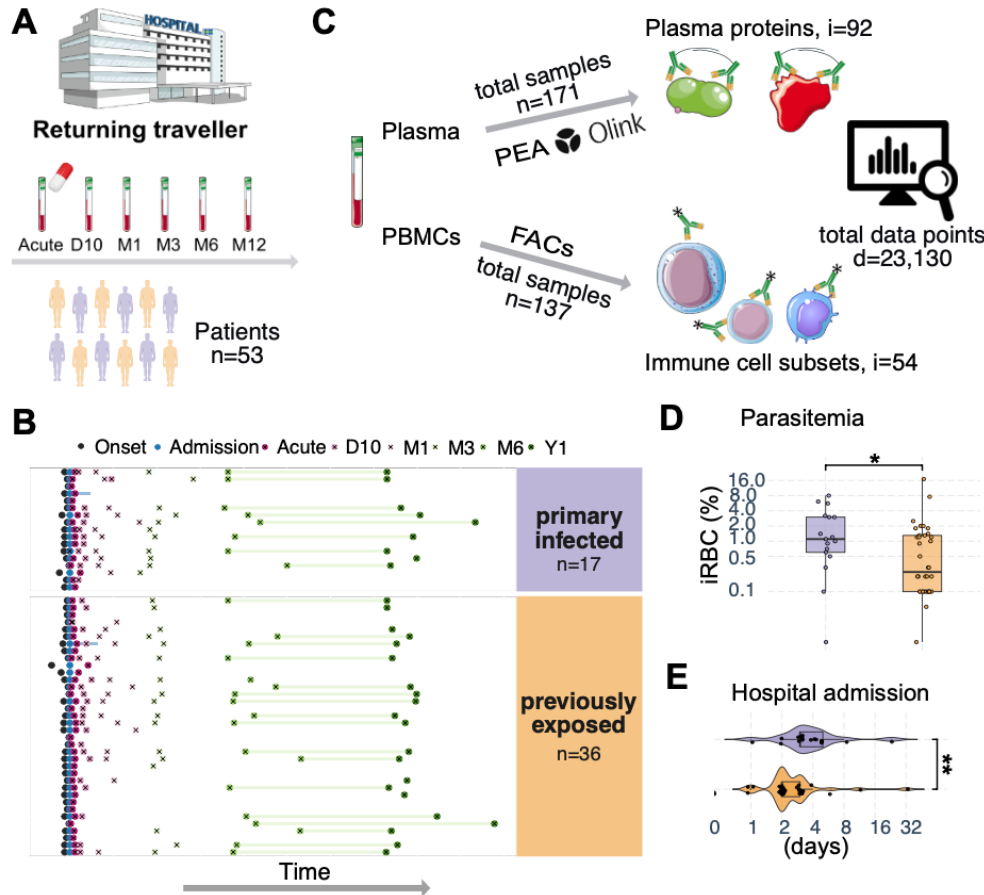
85 Subhead 1: Longitudinal profiling of peripheral blood – Immune dynamics after natural 86 infection in a cohort of returning travelers

87 We aimed to comprehensively profile the immune response dynamics longitudinally after natural
88 infection with *P. falciparum* malaria, to appreciate the immunological changes occurring during
89 the acute disease and up to one year after diagnosis. We included 53 returning travelers, repeatedly
90 sampled in a non-endemic setting over one year after hospital admission (13–16) (Fig. 1A).

91 To profile the immune response in the cohort over time, we performed broad FACS-based
92 immunophenotyping using a 17-marker panel and gated for subsets of monocytes (CD14⁺), T cells
93 (CD3⁺CD56⁻), and NK cell (CD3⁻CD56⁺) (Fig. S1A). We also included data from B cell subsets
94 previously phenotyped from the same donors (16) (Fig. S1B). Plasma protein analysis was
95 performed using the Target 96-plex Inflammation panel from Olink Proteomics (17) targeting 92
96 immune response-related proteins. In total, we profiled 182 samples from 53 subjects, creating
97 more than 23,000 data points (Fig. 1B).

98 The cohort consisted of individuals infected with *P. falciparum* malaria for the first time (primary
99 infected, n = 17) and those infected before, having grown up in malaria endemic areas and reported
100 previous malaria (previously exposed, n = 36) (Fig. 1C). Comparing individuals with primary
101 infection versus previous exposure enabled us to investigate potential memory effect on the
102 immune response. The individuals with previous exposure moved from malaria endemic areas to
103 non-endemic Sweden on average 11.5 years before now experiencing acute malaria after visiting
104 an endemic area (median = 11.5, range 0-46 years, Tab. S1).

105 Although all individuals sought healthcare, primary infected patients had significantly higher
106 levels of parasitemia at hospital admission (median 1.10 vs 0.25 % infected red blood cells, p =
107 0.038, Fig1D), more signs of severe malaria (Tab. S1) and were on average admitted to hospital
108 care significantly longer than previously exposed patients (median 3 vs 2 days, p = 0.002, Fig1E,
109 Tab. S1).



110

111 **Fig. 1. Systems level profiling of peripheral blood from individuals of a prospective cohort of**
 112 **returning travelers with *P. falciparum* malaria. (A) Overview of prospective longitudinal malaria**
 113 **cohort of returning travelers, (B) temporal sample information symptom onset (black), admission**
 114 **to Karolinska University Hospital (blue), six sampling time points (x) for immune profiling (acute,**
 115 **after 10 days, 1 month, 3 months, 6 months, 1 year) and convalescence average (green lines).**
 116 **Patients with primary infection (n = 17) are colored in purple, and patients with previous malaria**
 117 **exposure (n = 36) are colored in orange. (C) A total of 53 returning travelers were longitudinally**
 118 **profiled for plasma proteins using Olink Proteomics PEA platform (n = 171 samples, i = 92**
 119 **proteins) and their PBMC immune cells (n = 137 samples, i = 54 subsets), generating 23,130**
 120 **unique data points. Comparison of (D) parasitemia at diagnosis (percentage of infected red blood**
 121 **cells) and (E) length of hospital admission (days) for primary infected and previously exposed**
 122 **individuals. Statistical differences between groups were assessed using the non-parametric**
 123 **Wilcoxon-test. *p < 0.05, **p < 0.01.**

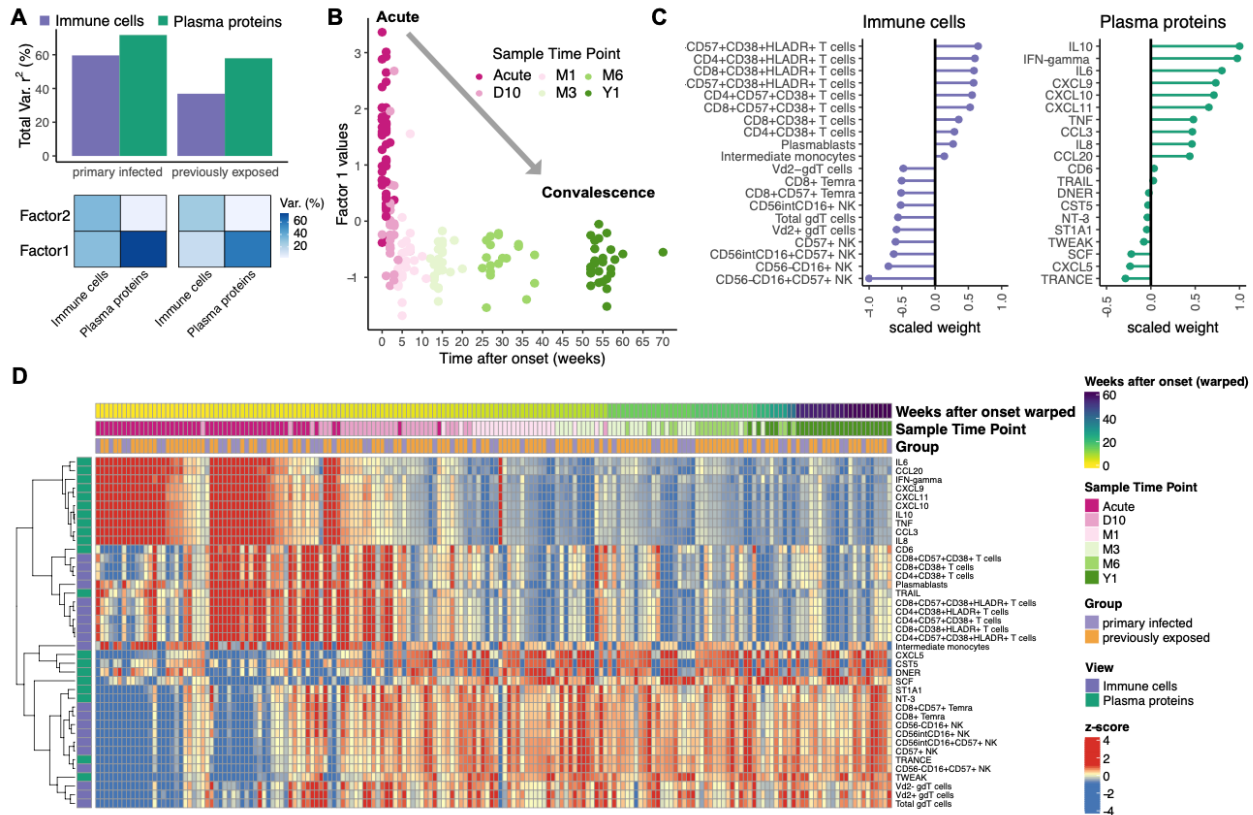
124

125 **Subhead 2: Integrated analysis of immune response on time axis after symptom onset**

126 To explore the immune response dynamics after natural *P. falciparum* malaria on a systems level
127 and in a data driven manner, we used multi-omics factor analysis (MOFA). The unsupervised
128 nature of MOFA allows the model to capture both biological and technical variability in the low-
129 dimensional factors space (18, 19). Here we used MEFISTO, a recent extension of MOFA which
130 allows for multi-omics integration of data while controlling for time-dependent variance in
131 repeated samples (20). MOFA can disentangle the sources of heterogeneity in diverse data types
132 and accept missing data points using matrix factorization (Fig. S2A). Using MEFISTO, the dataset
133 was described by two latent factors. These factors explained 37% to 60% and 58% to 72 % of the
134 immune cell subset and plasma protein dynamics, respectively (Fig. 2A). Factor1 was primarily
135 associated with time-dependent changes in the immune response to the infection (Fig. 2B and
136 S2B). Positive factor values were associated with the acute phase and negative factor values were
137 associated with the time after treatment and transition towards convalescence (Fig. 2B and S2C).
138 The positive factor values were driven by increased levels of IL10, pro-inflammatory cytokines
139 such as IFN-gamma, IL-6, TNF, CCL3, IL8, CDCP1, and chemokines such as CXCL9, CXCL10,
140 CXCL11. For immune cells, CD4⁺ and CD8⁺ T cells expressing activation markers CD38 and
141 HLA-DR, intermediate monocytes (CD14⁺CD16⁺) and plasmablasts
142 (CD19⁺CD20^{lo}CD38^{hi}CD27^{hi}) were associated with Factor1 (Fig. 2C). The negative factor values
143 were associated with the transition phase towards convalescence. Here, several subsets of NK cells
144 expressing CD57, CD8 T effector memory cells, and $\gamma\delta$ T cells were variables driving Factor1 for
145 the cellular immune response after treatment (Fig. 2C). We confirmed the accuracy of the model
146 parameters by comparing measured data between the acute and convalescent samples (internal
147 control; Fig. S2C-F) and to healthy control samples (external control; Fig. S3A-D).

148 We then used the integrated MEFISTO model to impute missing data points (plasma proteins data
149 modality, n = 11; immune cell modality, n = 64; Fig. S2A) to generate a heatmap of the integrated
150 immune landscape, visualizing the longitudinal immune system dynamics after disease. The
151 landscape dynamics, show a rapidly contracting pro-inflammatory response after treatment with a
152 temporary increase in primarily activated T cell subsets followed by a transition into a more long-
153 term post-infection response (Fig. 2D and Fig. S3).

154 In summary, our integrated analysis of immune cell subsets and plasma protein data after symptom
 155 onset allows us to draw a data driven descriptive immune landscape, describing the transition from
 156 the clinical acute phase towards convalescence over one year.
 157



158
 159 **Fig. 2. Integrated analysis of immune response dynamics for one year after malaria.** Integrated
 160 multi omics factor analysis method for the Functional Integration of Spatial and Temporal Omics
 161 data (MEFISTO) model was utilized to integrate data modalities, plasma proteins and manually
 162 gated cell subsets, respectively, with their temporal covariate of time after symptom onset. (A)
 163 Variance explained by the MEFISTO model. Differences due to previous parasite exposure were
 164 assigned to groups in order to model group-specific time-dependent immune response dynamics.
 165 (B) Plotting Factor1 value against the time after symptom onset (weeks) highlights the captured
 166 variance in Factor1 with positive factor values associated with acute phase samples and negative
 167 factor values associated with non-acute phase samples. (C) Top10 features of Factor1 for each of
 168 the immune system views based on negative and positive scaled feature weights - immune cells
 169 (purple) and plasma proteins (green). (D) The heatmaps visualize immune response dynamics for

170 *Factor1 driving features. The characteristic immune variables for each data modality, aligned to*
171 *time after symptom onset, reveals contrasting patterns characterizing the transition from acute*
172 *phase towards convalescence. Missing data points have been imputed based on model Factor1.*
173 *Cell counts and relative protein levels are shown as rows, and each column represents an*
174 *individual patient. Rows were clustered using Euclidean distance and column were arranged*
175 *according to MEFISTO model group-aligned time after onset. Cell counts and protein level values*
176 *were converted to z-scores.*
177

178 **Subhead 3: Relationship between acute cytokine milieu and cellular response**

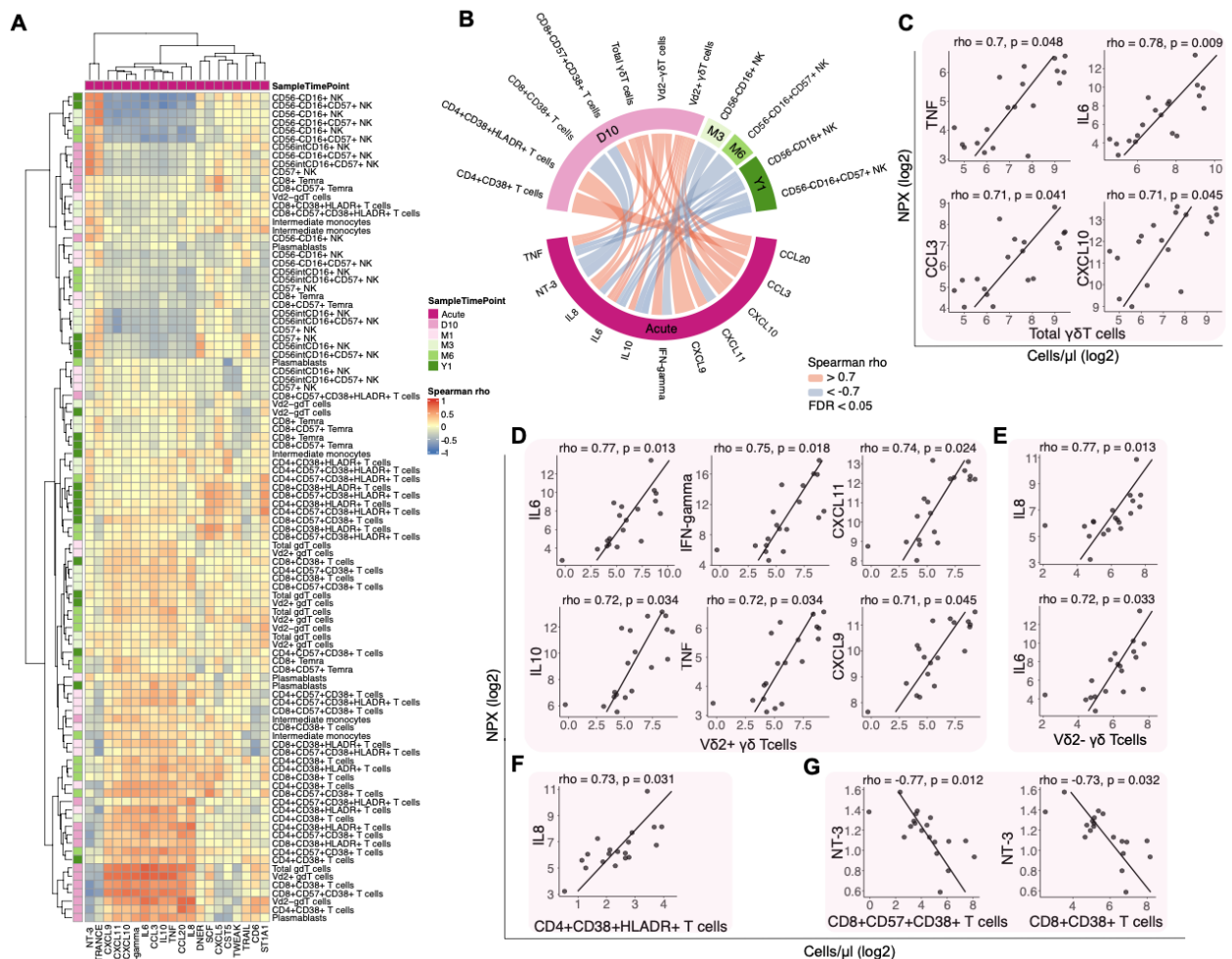
179 Cytokines and chemokines are known to orchestrate an immunological response to drive
180 recruitment, activation, and subsequently proliferation of immune cell populations. Hence, we
181 sought to analyze possible associations between levels of the acute phase responses and immune
182 cells subsets, characterizing the transition from acute towards convalescence.

183 Focusing on the top immune variables determined by the integrated model, we correlated acute
184 samples with all remaining sample time points using spearman rank correlation (Fig. 3A). We
185 discovered strong and significant correlations ($|\rho| > 0.7$, after adjusted FDR < 0.05) between
186 acute phase cytokines and immune cell subsets at all sample time points after treatment (D10, M3,
187 M6 and Y1) (Fig. 3B).

188 In particular, the numbers of $\gamma\delta$ T cell subsets at the 10-day sample time-point were strongly
189 associated with several pro-inflammatory cytokines at the acute time-point. The total level of
190 $\gamma\delta$ T cells positively correlated with TNF ($\rho = 0.704$, $p = 0.049$), IL6 ($\rho = 0.781$, $p = 0.009$),
191 CCL3 ($\rho = 0.712$, $p = 0.041$), and CXCL10 ($\rho = 0.707$, $p = 0.045$) (Fig. 3C). Especially the
192 $V\delta 2^+$ subset of $\gamma\delta$ T cells has been shown to be important in the immune response to malaria
193 parasites (21–23). When investigating these subsets, we observed that the number of $V\delta 2^+$
194 $\gamma\delta$ T cells was positively correlated with levels of IL6 ($\rho = 0.767$, $p = 0.013$), IFN-gamma (ρ
195 $= 0.753$, $p = 0.018$), CXCL11 ($\rho = 0.74$, $p = 0.024$), IL10 ($\rho = 0.723$, $p = 0.034$), TNF ($\rho =$
196 0.724 , $p = 0.034$), and CXCL9 ($\rho = 0.707$, $p = 0.045$) (Fig. 3D). The number of $V\delta 2^-$ $\gamma\delta$ T cells
197 in contrast was only positively correlated with levels of IL8 ($\rho = 0.77$, $p = 0.013$), and IL6 (ρ
198 $= 0.72$, $p = 0.033$) (Fig. 3E).

199 Acute phase levels of IL8 were also positively correlated with the number of activated
 200 (CD38⁺HLA-DR⁺) CD4⁺ T cells ($\rho = 0.728$, $p = 0.031$) at the 10-day sample time-point. In
 201 contrast, neurotrophin-3 (NT-3) levels were negatively correlated with the number of activated
 202 CD8⁺ T cells in several different subsets (CD57⁺CD38⁺; $\rho = -0.77$, $p = 0.012$ and
 203 CD57⁺CD38⁺HLA-DR⁺; $\rho = -0.726$, $p = 0.042$) (Fig. 3F, G).

204 These results point towards a strong association of the levels of pro-inflammatory cytokines during
 205 the early acute phase and the size of immune cell subsets after the acute phase. The highest degree
 206 of association was identified for $\gamma\delta$ T cells, and especially the V δ 2⁺ subset, which was strongly
 207 positively correlated with the levels of pro-inflammatory cytokines.



208
 209 **Fig. 3. Associations of the acute phase plasma protein response with immune cell subsets. (A)**
 210 **Heatmap based on overall Spearman correlation (ρ) acute phase plasma proteins and post-**

211 acute phase cell immune cell subsets. Blue and red colors symbolize positive and negative
212 correlations, respectively. **(B)** Chord diagram based on strong ($\rho > |0.7|$) and significant
213 correlations values (after adjusted FDR < 0.05). **(C-G)** Scatter plots to show acute phase plasma
214 protein levels and immune cell subset counts at day 10 post disease for significant correlations of
215 **(C)** Total $\gamma\delta$ T cells, **(D)** $V\delta 2^-$ $\gamma\delta$ T cells, **(E)** $V\delta 2^+$ $\gamma\delta$ T cells, **(F)** activated $CD4^+$ T cells and **(G)**
216 activated $CD8^+$ T cells. All stated p -values are FDR corrected for multiple testing.

217

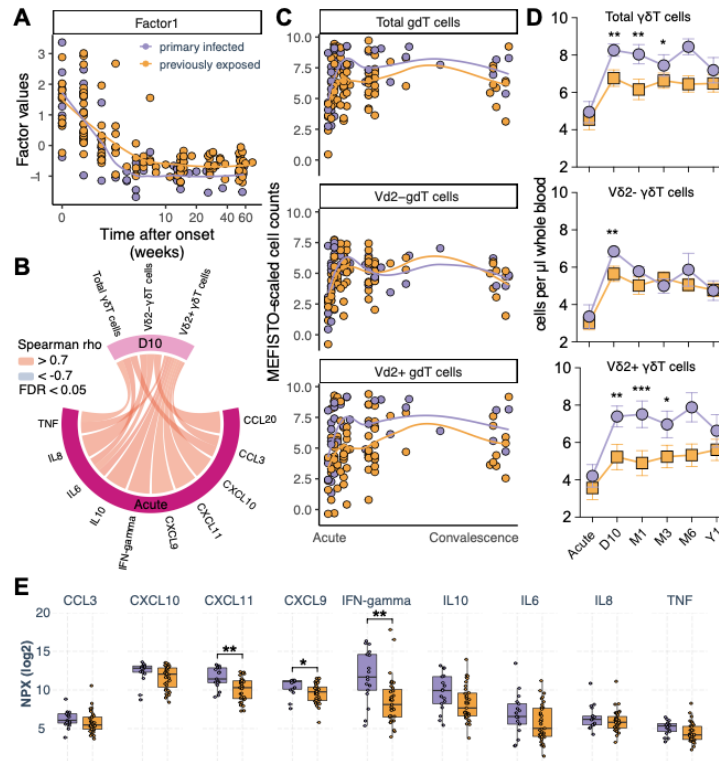
218 **Subhead 4: Impact of previous *P. falciparum* exposure on $\gamma\delta$ T cell responses**

219 To further characterize the association between acute phase cytokine levels and the $\gamma\delta$ T cell
220 response, we sought to examine if previous exposure to malaria parasites impacts this association.
221 Overall, both groups show similar trajectories of their immune dynamics when plotting Factor1
222 values against time (Fig. 4A). However, primary infected individuals were associated with both
223 higher and lower factor values during the acute phase and convalescent phase, respectively (Fig.
224 S2C). This indicates differences in protein and immune cell subset magnitudes attributed to
225 previous malaria.

226 Due to the strong correlation of acute phase proteins and $\gamma\delta$ T cell subset numbers at day 10 (Fig.
227 4B, excerpt of Fig. 3B), we aimed to investigate the association further in the context of previous
228 exposure.

229 When plotting $\gamma\delta$ T cells against the time after symptom onset, we observed that $V\delta 2^+$ $\gamma\delta$ T cells
230 expanded to a greater extent in primary infected individuals while $V\delta 2^-$ $\gamma\delta$ T cells expanded
231 similarly for both groups (Fig. 4C). We confirmed that especially the $V\delta 2^+$ subset was significantly
232 more expanded after the acute time-point in primary infected individuals (Fig. 4D). All acute phase
233 proteins that correlated with $V\delta 2^+$ $\gamma\delta$ T cells (Fig. 4B) followed a similar trend, although only IFN-
234 gamma, CXCL9 and CXCL11 were significantly higher in primary infected compared to
235 previously exposed individuals (Fig. 4E).

236 Here, we could show that primary infected individuals have significantly higher levels of pro-
237 inflammatory cytokines at the acute phase, as well as a significantly larger expansion of
238 $V\delta 2^+$ $\gamma\delta$ T cells after the acute phase compared with individuals previously exposed to malaria.



239

240 **Fig. 4. Impact of previous *P. falciparum* exposure on immune dynamics after clinical malaria.**

241 **(A)** Smooth fit of MEFISTO Factor1 values against time after symptom onset in weeks visualizing

242 transition from acute to convalescence for primary infected (purple) and previously exposed

243 (orange) individuals. **(B)** Associated inflammatory signature with $\gamma\delta$ T cells based on spearman

244 rank correlation. **(C)** $\gamma\delta$ T cell dynamics over time after symptom onset. **(D)** Longitudinal $\gamma\delta$ T cell

245 levels. Statistical differences between groups for $\gamma\delta$ T cell subtypes were assessed using linear

246 mixed model fit with restricted maximum likelihood and t-tests with FDR correction for multiple

247 testing. Error bars denote standard error of the mean. **(E)** Comparison between primary infected

248 (purple) and previously exposed (orange) individuals for acute phase proteins significantly

249 associated with $\gamma\delta$ T cells at the acute time-point. Statistical differences between groups were

250 assessed using the non-parametric Wilcoxon-test, FDR adjusted p-values to correct for multiple

251 testing. * $p < 0.05$, ** $p < 0.01$, *** $p < 0.001$.

252

253 **Subhead 5: Effect of previous malaria exposure on Vδ2⁺ $\gamma\delta$ T cell characteristics**

254 The V δ 2⁺ subset of $\gamma\delta$ T cells have been shown to play an important role in combating blood stage
255 malaria, via TCR-induced cytotoxicity and CD16 mediated phagocytosis (24, 25). We therefore
256 focused on characterizing the CD16⁺V δ 2⁺ $\gamma\delta$ T cell response further using linear-mixed effects
257 models to assess the impact of previous exposure to parasites on $\gamma\delta$ T cell functional markers.

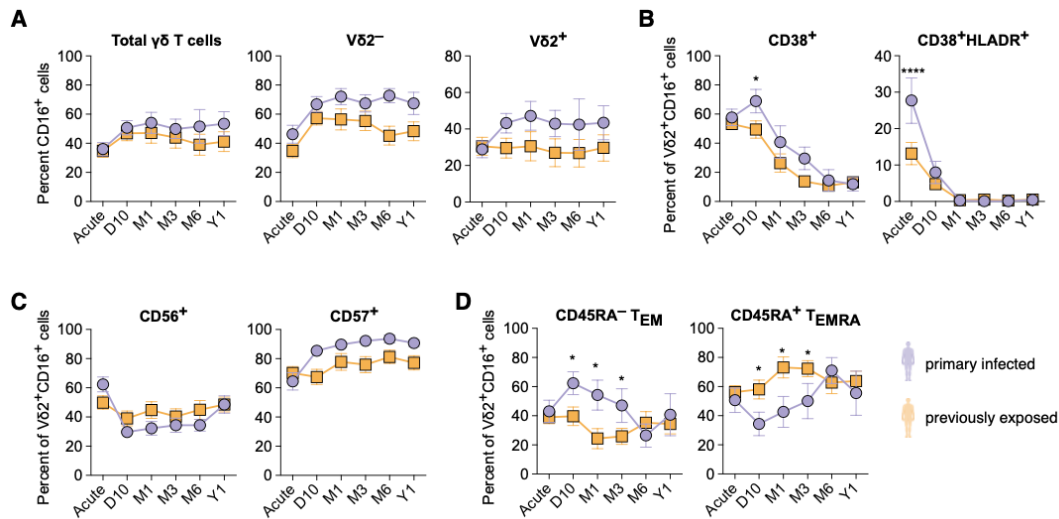
258 First, we assessed CD16 expression among $\gamma\delta$ T cells. The expression was similar between primary
259 infected and previously exposed individuals for total and V δ 2 positive and negative subsets (Fig.
260 5A). The frequency of CD16⁺ cells increased somewhat in both groups between the acute time-
261 point and 10 days, for V δ 2⁻ cells. A similar expansion was also observed for the V δ 2⁺ cells, but
262 only in primary infected individuals (Fig. 5A), potentially reflecting an upregulation in response
263 to infection. To further assess if the V δ 2⁺ $\gamma\delta$ T cells responded to the infection, we next investigated
264 the activation status of the CD16⁺V δ 2⁺ $\gamma\delta$ T cells. Approximately 60 % of all V δ 2⁺ $\gamma\delta$ T cells had
265 upregulated the activation marker CD38 at the acute infection. The primary infected individuals
266 then retained a significantly higher frequency of CD38⁺ cells at the day 10 time-point after which
267 the levels reduced over 3-6 months until reaching baseline levels (Fig. 5B). The increased
268 activation-status in primary infected individuals was also reflected by a significantly higher co-
269 expression of CD38 and HLA-DR at the acute time-point (Fig. 5B).

270 We also assessed the expression of CD56 and CD57, associated with NK cell cytotoxicity (26)
271 and replicative senescence (27), respectively. Although there were no differences between the
272 groups, there were some changes in cells expressing the markers over time, such as a temporary
273 reduction in the frequency of CD56⁺ cells after the acute infection, while CD57⁺ cells increased
274 over time (Fig. 5C). These effects were especially observed in primary infected individuals,
275 potentially reflecting the stronger $\gamma\delta$ T cell response in these individuals.

276 To further determine which subsets of V δ 2⁺ $\gamma\delta$ T cells that responded during infection, we assessed
277 the levels of CCR7 and CD45RA to identify different naïve or effector populations (28). Almost
278 all CD16⁺ V δ 2⁺ $\gamma\delta$ T cells were negative for CCR7 (median 98 % over all time-points), indicating
279 that these cells display an effector-phenotype. During the acute phase of the response, both groups
280 displayed similar distribution of effector memory (T_{EM}, CD45RA⁻) and T_{EMRA} (CD45RA⁺)
281 $\gamma\delta$ T cells (Fig. 5D). However, as the number of V δ 2⁺ $\gamma\delta$ T cells expanded in primary infected
282 individuals the frequency of effector memory cells significantly increased, while the frequency in

283 previously exposed individuals was relatively stable over time. This suggests that it was primarily
 284 effector memory $V\delta 2^+$ $\gamma\delta$ T cells that expanded after the acute infection.

285 Collectively these results show that despite $V\delta 2^+$ $\gamma\delta$ T cells only expanding in primary infected
 286 individuals, the cells became activated in both groups after infection. The level of activation and
 287 subsequent changes in host effector and differentiation markers were however different with a
 288 more robust effect in primary infected individuals.



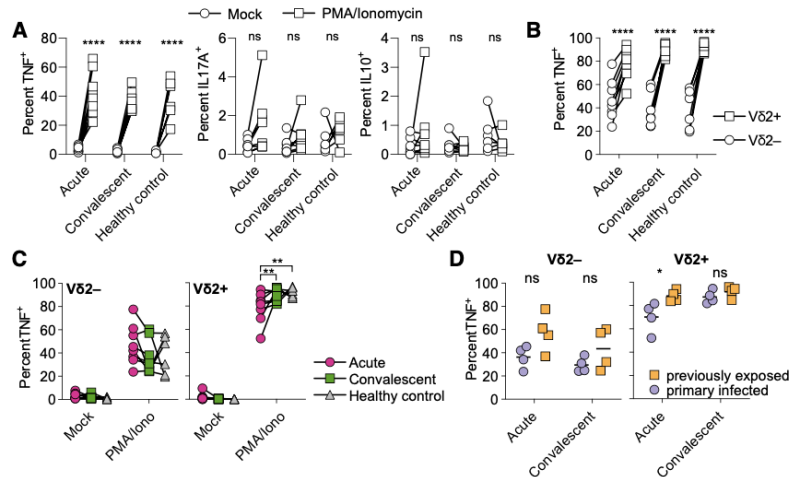
289
 290 **Fig. 5. Previous *P. falciparum* exposure impacts $\gamma\delta$ T cell expansion.** Linear mixed effect
 291 modelling by maximum likelihood for $\gamma\delta$ T cell frequencies for primary infected (purple) and
 292 previously exposed (orange) individuals, error bars denote the standard error of the mean. (A)
 293 Percentage of CD16+ cells of total $\gamma\delta$ T cells, $V\delta 2^-$ or $V\delta 2^+$ $\gamma\delta$ T cells. (B) Percent of $V\delta 2^+$ CD16+ $\gamma\delta$
 294 T cells expressing activation markers CD38 alone or together with HLA-DR. (C) Percent of $V\delta 2^+$
 295 CD16+ $\gamma\delta$ T cells expressing CD56+ or CD57+ (D) $V\delta 2^+$ $\gamma\delta$ T cells effector memory (CD45RA-) or
 296 T_{EMRA} (CD45RA+). Difference in cell frequency at each time point was evaluated by repeated t-
 297 tests with FDR correction. * $p < 0.05$, **** $p < 0.0001$.

299 **Subhead 6: $\gamma\delta$ T cell function is retained while expansion is affected due to previous**
 300 **malaria exposure**

301 It has been described that especially $V\delta 2^+$ $\gamma\delta$ T cells respond strongly during malaria but that this
 302 effect is reduced upon subsequent infections (29). This pattern is supported by our data, as the
 303 $V\delta 2^+$ $\gamma\delta$ T cell activation and especially expansion were reduced in previously exposed compared

304 to primary infected individuals (Fig. 4D). Previous descriptions indicate that the reduced
305 responsiveness can be due to changes in the imprinting through changes in the methylation patterns
306 (30, 31), although it remains unclear if such imprinting can last for this long. To assess if the
307 function of the $\gamma\delta$ T cells in our cohorts were inherently affected in their capacity to respond to
308 stimulation, we performed blinded cultures of PBMCs from primary infected and previously
309 exposed individuals. We stimulated the cells with PMA and ionomycin that together bypass the T
310 cell receptor complex and measured production of TNF α , IL17, and IL10. PMA and ionomycin
311 stimulation led to increased production of TNF α , but not IL17 or IL10 (Fig. 6A). Comparing the
312 response of V δ 2⁺ and V δ 2⁻ $\gamma\delta$ T cells, the V δ 2⁺ cells responded with more TNF α production (Fig.
313 6B), consistent with a proinflammatory effector function. For V δ 2⁻ $\gamma\delta$ T cells, the production of
314 TNF α was similar between the acute and convalescent time-point and healthy controls. For V δ 2⁺
315 $\gamma\delta$ T cells, however, the frequency of TNF α producing cells was reduced during the acute response,
316 but then recovered at the convalescent phase, for which frequencies were similar as in healthy
317 controls (Fig. 6C). Further separating the V δ 2⁺ and V δ 2⁻ subsets into primary infected and
318 previously exposed individuals showed no differences between the groups for V δ 2⁻ cells, while
319 primary infected individuals responded with lower numbers of TNF α -producing V δ 2⁺ cells at the
320 acute time-point (Fig. 6D), potentially reflecting a larger proportion of already activated cells being
321 restimulated.

322 In summary, V δ 2⁺ $\gamma\delta$ T cells from previously exposed individuals do not display apparent intrinsic
323 dysfunctionality upon *ex vivo* reactivation. This further supports a role for extrinsic factors
324 regulating V δ 2⁺ $\gamma\delta$ T cell activation and expansion in malaria.



325

326 **Fig. 6. $\gamma\delta$ T cell function in response to restimulation.** (A) PBMCs from donors with primary
 327 infection ($n = 4$) and previous parasite exposure ($n = 4$) at the acute and convalescent time-point
 328 (6-12 months after infection) and healthy controls ($n = 6$) were stimulated with PMA and
 329 ionomycin (open boxes) or left unstimulated (Mock, open circles) for 5 hours. Frequencies of
 330 TNF α , IL17A, and IL10-producing cells were then measured. (B) TNF α cells were compared
 331 between V δ 2 $^{+}$ (open boxes) and V δ 2 $^{-}$ (open circles) cell subsets. (C) Comparison of TNF α
 332 frequencies in V δ 2 $^{-}$ and V δ 2 $^{+}$ cell subsets at the acute time-point (pink circles), convalescent time-
 333 point (green boxes) and healthy controls (grey triangles). (D) Comparison of TNF α V δ 2 $^{-}$ and V δ 2 $^{+}$
 334 cells between primary infected (purple circles) and previously exposed (orange boxes) individuals.
 335 Statistical comparisons for A-C were done using a matched pair two-way ANOVA followed by
 336 Tukey's post-hoc test, while statistics in D was evaluated by two-way ANOVA followed by Sidak's
 337 post-hoc test. * $p < 0.05$, ** $p < 0.01$, **** $p < 0.0001$, ns = not significant.

338

339 Subhead 7: Acute malaria specific IgG3 levels are associated with the level of inflammation 340 and $\gamma\delta$ T cell expansion

341 A long-lived memory imprint to pathogenic encounter is in general mediated by the adaptive
 342 immune system. Here, we report that previously exposed individuals without re-exposure to
 343 parasites for many years (average 11.5 years since leaving an endemic region), at the time of a
 344 new acute infection respond with a reduced pro-inflammatory cytokine response upon re-infection
 345 as well as reduced V δ 2 $^{+}$ $\gamma\delta$ T cell expansion. Hence, we hypothesized that the reduced pro-

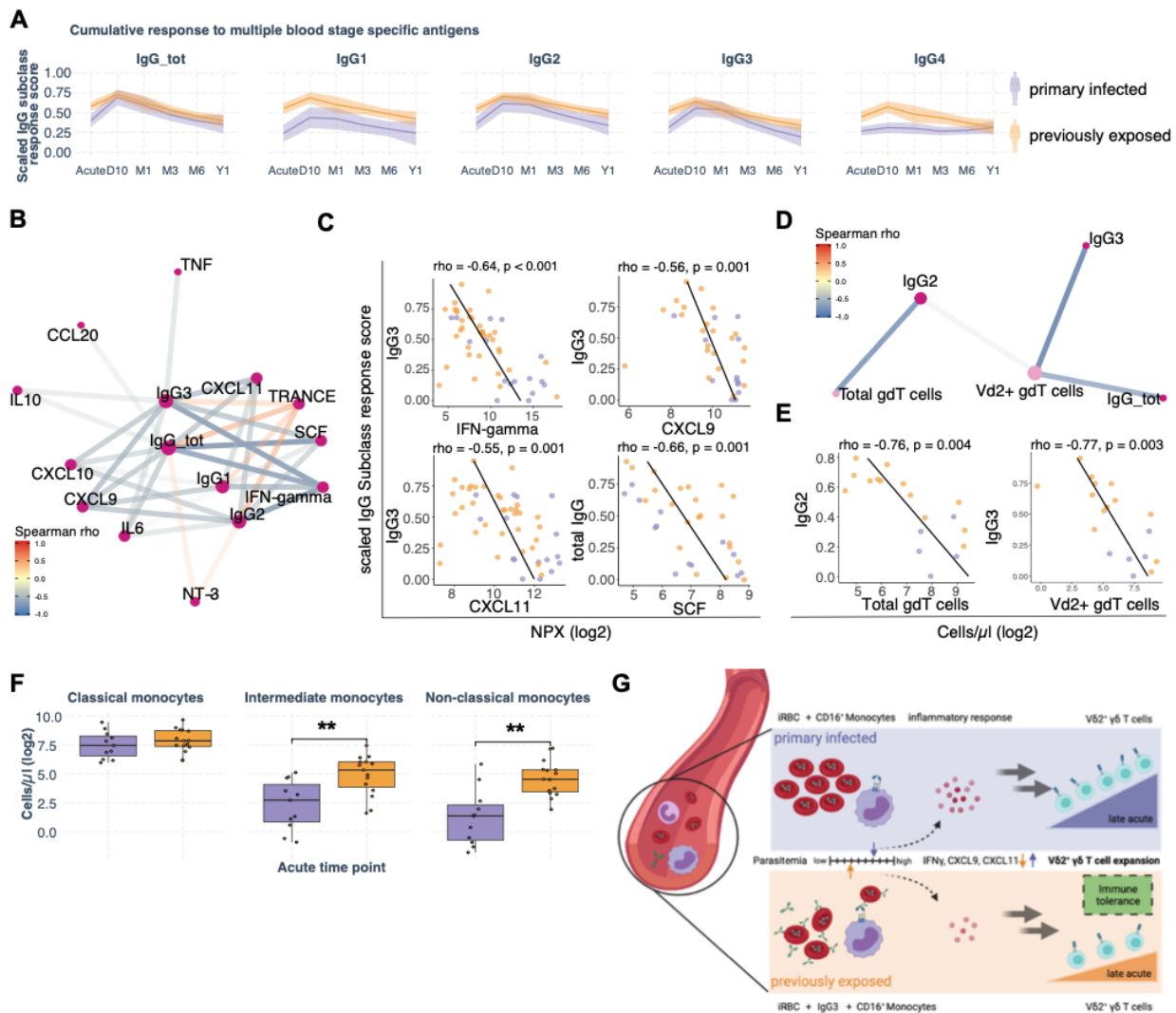
346 inflammatory response and $\gamma\delta$ T cell expansion could be mediated by existing long-lived adaptive
347 humoral immune memory responses.

348 To investigate this, we repurposed a previously published dataset, investigating the
349 immunoglobulin G subclass response (IgG1-4) to five malaria *P. falciparum* blood-stage antigens
350 (AMA1, MSP1, MSP2, MSP3, and RH5) in 51 matching individuals from the same cohort (15).
351 We established an IgG subclass and time point specific score, the cumulative response score (CRS)
352 that summarizes the responses to the separately measured malaria specific antigens from the
353 previous study (Fig. S5). The CRS dynamics correspond to the average breadth of the antibody
354 response for total IgG and IgG subclasses (Fig. 7A).

355 Spearman rank correlation showed that levels of several acute pro-inflammatory cytokines were
356 strongly inversely correlated with IgG subclass CRS (Fig.7B), in particularly IgG3 and IFN-
357 gamma levels (Fig. 7C). The IgG2 and IgG3 subclass CRSs at the acute infection were also
358 negatively correlated with day 10 total and $V\delta 2^+$ $\gamma\delta$ T cell numbers, respectively (Fig. 7D), with
359 an especially strong negative correlation between IgG3 levels and $V\delta 2^+$ $\gamma\delta$ T cell numbers (Fig.
360 7E).

361 Cytophilic immunoglobulins such as IgG3 can interact with CD16 expressing immune cells,
362 including $\gamma\delta$ T cells, and intermediate ($CD16^+CD14^{high}$) and non-classical ($CD16^+CD14^{lo}$)
363 monocytes. Interestingly, we observed higher numbers of intermediate and non-classical
364 monocytes at the acute time point for previously exposed compared to primary infected individuals
365 (Fig. 7F). These observations, together with an increased IgG3 response, points towards an
366 antibody-phagocytosis mediated mechanism that could partly explain the lower parasitemia
367 observed in individuals with prior exposure to malaria parasites (Fig. 1E). To assess if this could
368 be the case, we used linear regression to determine which associated combinations of immune
369 factors that best explain the difference in expansion of $V\delta 2^+$ $\gamma\delta$ T cells for the two exposure groups.
370 Using Directed Acyclic Graphs (DAG) (32), we determined the minimal sufficient adjustment sets
371 of covariates for estimating the total effect of a given associated component on acute IFN-gamma
372 levels and day 10 $V\delta 2^+$ $\gamma\delta$ T cell numbers, respectively (described in Supplementary Methods and
373 Fig. S7). Comparing the reference model with exposure group as explanatory variable to the DAG-
374 based adjusted immune response component model, we concluded that the IFN-gamma response
375 was not directly explained by the parasitemia (Fig. S7A). In contrast, differences in $V\delta 2^+$ $\gamma\delta$ T cell

376 expansion was partly explained by parasitemia, but more directly by cytophilic antibody levels
 377 and CD16⁺ intermediate monocytes (Fig. S7B-C). This suggests a potentially more direct
 378 antibody-mediated effect by regulating cytokine levels. Based on these results we suggest a
 379 working model where early production of parasite-specific antibodies interact with innate immune
 380 cells to regulate parasitemia and cytokine levels, which in turn control subsequent $\gamma\delta$ T cell
 381 expansion (Figure 7G).
 382



383
 384 **Fig. 7. Adaptive response due to prior malaria exposure linked to dampened immune**
 385 **inflammation.** (A) Cumulative IgG subclass response score (CRS) to 5 blood-stage antigens from
 386 Yman et al., BMC Medicine, 2019, over sample time points for primary infected (purple) and

387 *previously exposed (orange) individuals (n = 52), shaded area denotes the 95% confidence*
388 *interval. (B) Correlation network of plasma proteins and IgG subclass CRS values at the acute*
389 *time-point, FDR corrected $p < 0.05$ (C) Scatter plots for significant correlations, FDR adjusted p -*
390 *values are stated. (D) Correlation network of acute IgG subclass CRS values and immune cell*
391 *subsets at the 10-day sample time point, FDR corrected $p < 0.05$, $\rho < -0.7$. (E) Scatter plots for*
392 *significant correlations, FDR corrected $p < 0.05$. (F) Cell counts of monocyte subsets at the acute*
393 *time point. Statistical differences between groups were assessed using the non-parametric*
394 *Wilcoxon-test, FDR adjusted p -values to correct for multiple testing. $*p < 0.05$, $**p < 0.01$ (G)*
395 *Schematic model to explain improved disease tolerance in previously exposed individuals.*

396 DISCUSSION

397 Immunity to malaria is slow to develop. It has been proposed that this is partly due to immune
398 perturbations during infection (41). Understanding how the immune system is affected during
399 natural infection with malaria parasites is important to identify the potential role of individual
400 immune mediators in this process. Here, we used systems immunology to comprehensively
401 investigate the immune landscape after natural malaria and over one year after infection in the
402 absence of re-exposure to parasites. By sampling each individual over time, we could reduce
403 potential noise associated with inter-individual variability in their immune response to the
404 infection. Overall, the integrated immune landscape identified the acute phase followed by a
405 transitional phase leading into convalescence up to one year after disease. The acute phase was
406 characterized by activated CD4⁺ and CD8⁺ T cells and high levels of inflammatory cytokines and
407 chemokines, consistent with previous literature (2, 33). Here, a comprehensive analysis of immune
408 components over time revealed that acute inflammatory response signature associated with long-
409 term changes to cellular immune response.

410
411 The composition of our cohort, consisting of both primary infected and previously exposed
412 individuals, allowed us to study the impact of memory on the acute response and its associations
413 with the transition towards immunological convalescence. We could show that previously exposed
414 individuals produce lower levels of pro-inflammatory cytokines during natural *P. falciparum*
415 infection. Similar findings have been observed at the blood transcriptome level by Tran et al.,
416 where Malian adults exhibited a dampened inflammatory response compared to first time CHMI-
417 infected Dutch adults (34). Further, a study from a cohort of children in Uganda showed that older
418 children have lower levels of serum cytokines during acute malaria compared to younger children
419 (35). These previous studies, together with our findings of reduced pro-inflammatory response
420 confirms that previous malaria exposure, possibly cumulative, induces a form of tolerance
421 response. Of note, all individuals in our cohort experienced clinical malaria, suggesting that the
422 level of tolerance could be dependent on the amount of prior exposure to the parasite. However,
423 the individuals with previous exposure had left malaria endemic areas on average 11.5 years earlier
424 before being reinfected/experiencing a new episode of acute *P. falciparum* malaria after visiting
425 endemic area, indicating that the mechanism is significantly long-lived.

426

427 Antibodies are highly associated with protection from malaria and a key building block of naturally
428 acquired immunity. We have recently reported that previously exposed individuals from our cohort
429 responded to infection by producing high levels of *P. falciparum*-specific IgG, particularly of the
430 cytophilic subclasses IgG1 and IgG3 (15). Memory B cells and long-lived plasma cells constitute
431 a likely source of the increased parasite specific antibodies (15, 36), as memory can be maintained
432 for up to 16 years without re-exposure in a different cohort of travelers (37). Re-purposing the
433 previously published antibody data (15) enabled us to link the effect of adaptive responses, in the
434 form of an increased cytophilic antibodies, to enhanced functionality of the innate response. As
435 reported here, previously exposed individuals responded to malaria with an overall dampened
436 inflammatory response but significantly higher numbers of intermediate monocytes (38). Their
437 expression of CD16 (FcγRIII), a receptor for cytophilic antibodies of the subclasses IgG1 and
438 IgG3, can mediate parasite clearance through antibody-dependent phagocytosis (ADP) and/or
439 antibody-dependent cellular cytotoxicity (ADCC) (39). Indeed, higher numbers of CD16⁺
440 monocytes and a stronger IgG3 response against blood stage antigens indicate an interplay which
441 could promote lower levels of parasitemia, compared to individuals without previous exposure.
442 Supporting such a mechanisms, vaccination with RTS,S/AS01 leads to CD16-mediated
443 phagocytosis associated with protection (40).

444
445 We propose that antibody-mediated parasite control is an important component in shaping the pro-
446 inflammatory cytokine milieu towards a reduced pro-inflammatory response which could be
447 important for the development of immune tolerance (41). Complementary to the described
448 adaptive-innate interplay, several recent studies suggest that monocytes are modulated towards a
449 tolerance phenotype (5, 41). The mechanism of this imprint remains unclear, but a rodent model
450 point towards transcriptomic reprogramming of monocytes in the spleen (5), while data from *in-*
451 *vitro* stimulated monocytes from a cohort in Mali point towards epigenetic reprogramming of
452 myeloid progenitor cells in the bone marrow (41). However, to our knowledge, no study has shown
453 that epigenetic remodeling can remain and affect innate cells at re-stimulation for that long.

454 An alternative hypothesis, that overcomes the fact that monocytes have a short lifespan (42), is
455 that they are remodeled in their function due to constant stimuli by remaining hemozoin in the
456 spleen (5, 43, 44).

457 Both hypotheses of epigenetic imprinting and through splenic remodeling need further
458 investigation. In our cohort, where study participants moved away from malaria endemic areas 10
459 years prior, we propose an additional mechanism responsible for the tolerogenic response via the
460 interplay of innate and adaptive immunity. We suggest that tolerance develops over several
461 exposures to parasites and further that it is sustained long-term through adaptive memory
462 responses. However, these above hypotheses are not mutually exclusive and could potentially
463 synergize.

464

465 In agreement with previous reports, we observed expanding $\gamma\delta$ T cells after the initial inflammatory
466 response in response to the infection (45, 46). $\gamma\delta$ T cells are suggested to have an important role in
467 the control of malaria (29) and direct anti-parasite functions during the blood stage have been
468 reported (24). In this study, we observed that the acute phase inflammatory response was positively
469 associated with expansion of $V\delta 2^+$ $\gamma\delta$ T cells, and further that this was strongly impacted by
470 previous malaria exposure, resulting in a dampened inflammatory response and less $\gamma\delta$ T cell
471 expansion. Interestingly, this effect was primarily observed for the subset of $V\delta 2^+$ and not $V\delta 2^-$
472 $\gamma\delta$ T cells. The strong association could indicate that the pro-inflammatory response directly or
473 indirectly shapes the subsequent $\gamma\delta$ T cell expansion and capacity to adapt to prolonged and high
474 levels of blood stage parasitemia.

475

476 $V\delta 2^+$ $\gamma\delta$ T cells are known to activate and expand during a primary *P. falciparum* infection in
477 response to malaria phosphoantigens and that their activity is modulated upon subsequent
478 infections (47). Given the recently described role of $V\delta 2^+$ $\gamma\delta$ T cells in antiparasitic activities via
479 antibody-CD16 dependent phagocytosis of infected erythrocytes and cytotoxicity (24, 25),
480 associations to possible activity modulating factors are of interest. The benefit of reduced
481 expansion of $\gamma\delta$ T cells due to a dampened inflammatory response could be to reduce overall
482 inflammatory responses, which are otherwise potentially detrimental to the host (48). This is a
483 common hypothesis as the $\gamma\delta$ T cells are known to acquire a dysfunctional or tolerance phenotype
484 over time with repeated episodes of malaria (23). This reduction in $\gamma\delta$ T cell effector function was
485 associated with continuous malaria exposure (23), although it remains unclear what the
486 underlying tolerance mechanism is, and how long-lived such an effect could be. To assess if the

487 reduced activation and expansion of V δ 2⁺ γ δ T cells could be due to an inherent inability of the γ δ
488 T cells to respond, we re-stimulated cells from primary infected and previously exposed
489 individuals. However, we did not observe any reduced response that could have been associated
490 with intrinsic down-regulation of effector functions. Based on this, we instead hypothesized that
491 the regulation of V δ 2⁺ γ δ T cell activation and expansion was likely due to extrinsic mechanisms.
492

493 Among the cytokines and chemokines associated with V δ 2⁺ γ δ T cell expansion, we found IFN-
494 gamma and CXCL11 significantly reduced in previously exposed individuals. CXCL11 is
495 chemotactic for activated T cells, and it was reported that individuals with asymptomatic
496 *P. falciparum* malaria had lower levels in an endemic setting (49). IFN-gamma and the IFN-
497 gamma inducible chemokine CXCL9 are associated in a different context with regulatory crosstalk
498 of pro-inflammatory γ δ T cell effects (50), which could explain the association of these cytokines
499 with subsequent expansion. Consistent with these observations, both IFN-gamma and CXCL11
500 were reduced due to previous parasite exposure in a mouse model, suggesting some type of
501 memory response (5).

502
503 In summary, our results, together with previous research in the field, supports a model where early
504 control of host self-damage through increased tolerance is needed until a more broad, diverse, and
505 protective antibody repertoire is achieved (see Figure 7G). The tolerance response (dampened pro-
506 inflammatory response and reduced V δ 2⁺ γ δ T cell expansion) could be mediated in two ways: 1)
507 an expanding antibody repertoire that enhances CD16⁺ mediated phagocytosis and effector
508 functions, direct parasite neutralization and blocking further RBC invasion, rosetting and
509 sequestration by merozoites, and 2) training/priming during previous malaria episodes via
510 epigenetic or transcriptional remodeling of the monocyte population, potentially leading to rapid
511 generation of CD16-expressing monocytes with enhanced antibody effector functions.

512
513 From an evolutionary perspective, this type of dampened inflammatory response could be
514 important to generate an efficient B cell response, as recently shown in an influenza vaccine study
515 (51) and further supported by mouse models of malaria (52). Although further studies are needed
516 to evaluate these mechanisms on a cellular and molecular level, the comprehensive systems levels

517 analysis performed here provides a dynamic description for how proteins, cells, and antibodies,
518 interact in the host response to malaria during and after primary and repeated infection.
519

520 MATERIALS AND METHODS

521 Study design/cohort

522 A prospective study enrolling adult patients diagnosed with *P. falciparum* malaria at Karolinska
523 University Hospital in Stockholm, Sweden. Fifty-three patients that were admitted with acute
524 *P. falciparum* infection between 2011 and 2017, and where both cells and plasma was frozen were
525 included in the current study. We stratified the patients based on previous exposure to compare the
526 immune responses in malaria-naïve individuals of primarily Swedish origin, who contracted
527 malaria for the first time (n = 17, denoted as primary infected), with individuals originating from
528 malaria-endemic areas in Sub-Saharan Africa and reporting previous malaria (n = 36, denoted as
529 previously exposed). Patients were invited for sampling at the time of malaria diagnosis (Acute)
530 and then at approximately 10 days (D10), 1 month (M1), 3 months (M3), 6 months (M6), and 12
531 months (Y1) (see Fig.1A). On each sampling, venous blood was collected for plasma and serum
532 isolation, PBMC preparation and blood chemistry. Peripheral blood mononuclear cells (PBMCs)
533 were isolated using Ficoll-Paque density gradient separation, resuspended in 90 % fetal calf serum
534 supplemented with 10% DMSO, and stored at - 150°C. Clinical data was extracted from medical
535 records, and a questionnaire relating to the participant's health status, previous traveling, and
536 malaria exposure was filled in by all participants (Table S1).

537 Part of the cohort has been described previously for clinical (53), parasitological (13) and
538 immunological aspects (15, 16, 54).

539 In addition, we profiled peripheral blood samples of eight healthy controls to compare relative
540 measures of protein expression and cell populations with healthy/normal values (Figure S2).

541

542 Clinical diagnostics

543 *P. falciparum* parasites were detected and enumerated by light microscopy of Fields stained thick
544 and thin blood smears at the Department of Clinical Microbiology at Karolinska University
545 Hospital in addition to PCR as described previously (13). Leukocyte, neutrophil, monocyte, and
546 platelet cell differential counts were performed at the Department of Clinical Chemistry at
547 Karolinska University Hospital.

548

549 **Data acquisition**

550 **Immune cell phenotyping**

551 Immune cells were phenotyped by Flow cytometry (LSRFortessa, BD) and a panel of 17 antibodies
552 covering major immune cell populations and subpopulations (Fig. S1) for 137 samples. Frozen
553 PBMCs were thawed in a 37°C water bath and mixed with 1 equal volume cold Iscove's Modified
554 Dulbecco's Medium supplemented with L-glutamine (2 mM), penicillin (100 U/ml), streptomycin
555 (100 µg/ml), and 10 % heat-inactivated fetal bovine serum (all from Thermo Fischer Scientific).
556 Cells were then rested 20 minutes on ice before being washed twice in DPBS lacking magnesium
557 or calcium. After washing, the cells were incubated with Aqua Live/Dead stain (Thermo Fisher
558 Scientific) for 20 minutes followed by further washing in DPBS supplemented with 2% FBS. The
559 cells were then incubated for 20 minutes on ice, in 2 steps with 2 washes in between, using an
560 antibody mix targeting surface antigens (Table S2). After staining, the cells were washed twice in
561 DPBS with 2% FBS before acquisition on a 5-laser BD LSRFortessa flow cytometer. Gating was
562 done with FlowJo X software version 10.4.2, with the gating strategy shown in Figure S1.

563 **Plasma protein profiling**

564 Plasma proteins relevant for the immune response were profiled using the Proximity Extension
565 Assay (PEA) (Olink Proteomics, Sweden) to analyze 171 samples of 53 individuals using Olink
566 Target 96 Inflammation panel (92-plex). The method has been described previously (17). Briefly,
567 paired oligonucleotide-coupled antibodies bind to target proteins, leading to hybridization of the
568 oligonucleotides when the antibody-pair is in close proximity, forming a PCR template for real-
569 time PCR detection. Resulting data is normalized using assay internal controls and transformed
570 into Normalized Protein eXpression (NPX) values, representing an arbitrary relative quantification
571 unit on log₂ scale. After quality control and removal of markers with a missing frequency greater
572 than 50%, 74 proteins remained for downstream analysis.

573

574 ***In vitro* stimulation for detection of $\gamma\delta$ T cells cytokine production**

575 For intracellular staining, PBMCs were thawed, washed, resuspended in complete RPMI media
576 supplemented with 10% FCS and then incubated at 37°C over-night. The cells were then
577 stimulated with PMA (0.4 µM) and ionomycin (13 µM) per 10⁶ cells, (Nordic Biosite AB) for 5
578 hours. Golgi plug (BD Biosciences) was added after the first hour of stimulation. Activated cells
579 were subsequently stained with antibodies targeting the surface markers CD3, $\gamma\delta$ TCR, and V δ 2,

580 according to manufacturers' instruction. Cells were then fixed and permeabilized using the BD
581 Cytotfix/Cytoperm reagents (BD Biosciences) and stained with intracellular antibodies for TNF,
582 IL17A, and IL10 (Table S2). For the exclusion of dead cells, LIVE/DEAD aqua fixable viability
583 staining kit (Invitrogen) was used. Cells were acquired using a BD LSR Fortessa BD (BD
584 Biosciences) and the data analyzed using FlowJo Version 7.6 (FlowJo, Ashland, OH).

585 **Bioinformatics**

586 **Immune cell data normalization**

587 Prior to bioinformatic analysis, cell proportions from manually gates (Fig. S1) were normalized to
588 the number of cells per 1000 live cells. Subsequently, we adjusted the experimentally obtained live
589 cell counts with lymphocyte and monocyte counts from clinical blood chemistry counts for each
590 individual and timepoint to obtain cells per microliter blood values (Fig. S5A). Monocyte gates
591 containing values (Fig. S1A) were normalized according to:

$$592 \quad \frac{\text{cells}}{1000 \text{ live cells}} * (\text{lymphocyte counts} + \text{monocyte counts}) = \frac{\text{cells}}{\text{microliter blood}}$$

593 Values of pure lymphocyte containing gates (Fig. S1B) were normalized according to:

$$594 \quad \frac{\text{cells}}{1000 \text{ live cells}} * \text{lymphocyte counts} = \frac{\text{cells}}{\text{microliter blood}}$$

595 To standardize the cells-per-microliter values and to normalize the data set for extreme values, we
596 performed log₂ transformation. Standardized data was comparable to not-standardized data (Fig.
597 S5B).

598 **Antibody cumulative response score (CRS) calculation**

599 A previous study on individuals of the traveler cohort investigated the immunoglobulin G subclass
600 response (IgG1-4) s to five malaria *P. falciparum*-blood-stage antigens (AMA1, MSP1, MSP2,
601 MSP3, RH5) in 52 this current study matching cohort individuals (15). For the current study, we
602 though to look at the overall IgG subclass response to merozoite antigens instead of specific
603 antigens. To summarize the adjusted signals, measured for each antigen and each subclass, we
604 rank normalized the signals to achieve normal distribution for each antigen (Fig. S5A). Normally
605 distributed antigen response values were then summarized for each IgG subclass and time point,
606 creating the cumulative response score (CRS), presenting an average breadth value of the antibody
607 response for IgG subclasses (Fig. S5B).

608

609 **Statistical analysis and visualization**

610

611 **Multi-Omics-Factor Analysis**

612 Multi-Omics Factor analysis (MOFA) is a powerful tool for omics integration. It reduces high-
613 dimensional data into a few latent factors by capturing multi-dataset spanning variance in these
614 factors. The unsupervised nature of MOFA+ allows the model to capture both biological and
615 technical variability in the low-dimensional factors space (18, 19). A recent development
616 (MEFISTO) in addition allows for multi-omics integration of data with continuous structures given
617 by temporal relationships(20). Here, we utilized MEFISTO to analyze the underlying key drivers
618 for the time course of one year after infection on our cohort of returning travelers with
619 *P. falciparum* malaria.

620 For the data-driven-integration approach, we used 15,396 immune feature data points out of 23,130
621 possible. We included manually gated immune cell subset (features = 44) data and highly
622 multiplexed plasma protein data (features = 60) and including the time after symptom onset (0-70
623 weeks) for each sample to disentangle time dependent variation on a systems-level.

624 To standardize the actual time covariate of each sample, we used the time after reported symptom
625 onset for each sample as a temporal covariate for the model. Moreover, we assigned the time-
626 associated samples to groups of primary infected (n = 57) and previously exposed (n = 125) to
627 account for previous *P. falciparum* exposure. Immune parameters without temporal variation were
628 excluded prior to model training.

629 We trained the MEFISTO model using default model options, but adjusted training options (drop-
630 factor-threshold = 0.05; maxiter = 10,000; convergence_mode = slow). To align the covariates
631 across groups, warping was set “TRUE” and “primary infected” was set as warping reference
632 group. The optimal model was determined by the MOFA+ function run_mofa() with the setting
633 “use_basilisk = T”.

634

635 All data wrangling, analysis and visualization was done using R (www.r-project.org) using the
636 tidyverse package (55). Spearman correlation analysis with FDR/BH correction for multiple
637 testing (56) was done using the correlation package (57). If not stated otherwise, non-parametric
638 data distribution was assumed, and statistical difference was assessed using unpaired Wilcox Test
639 from rstatix (<https://github.com/kassambara/rstatix>).

640 Results were visualized using r packages circlize (58), complexHeatmap (59) and ggpubr
641 (<https://github.com/kassambara/ggpubr9>). Linear-mixed-effect models, with subjectID as random
642 effect, were fitted in GraphPad prism version 9.1.2 using restricted maximum likelihood followed
643 by t-tests using predicted least squares means with Benjamini and Hochberg FDR correction for
644 multiple testing (56).

645

646 **Supplementary Materials**

647 Table S1. Descriptive statistics prospective cohort of returning travelers.

648 Table S2. Staining panel for flow cytometry

649 Fig. S1. Flow cytometry manual gating strategy – T cell and B cell panel.

650 Fig. S2. MEFISTO model and cohort internal feature evaluation.

651 Fig. S3. Cohort external evaluation - comparison of plasma protein and PBMC profiles at Acute
652 and Y1 compared to healthy controls.

653 Fig. S4. Comparison of MEFISTO Factor1 values for exposure groups on time points.

654 Fig. S5. Cumulative Response Score for malaria antigen specific IgG subclass response of Yman
655 et al 2019 data set.

656 Fig. S6. Leukocyte count adjusted cell counts.

657 Fig. S7. Directed Acyclic Graphs – DAGs and linear regression

658

659 **References and Notes**

660 1. World Health Organisation, *World malaria report 2020* (Geneva, 2020);

661 <https://www.who.int/teams/global-malaria-programme/reports/world-malaria-report-2020>).

662 2. J. Langhorne, F. M. Ndungu, A. M. Sponaas, K. Marsh, Immunity to malaria: More questions
663 than answers *Nature Immunology* **9**, 725–732 (2008).

664 3. F. H. A. Osier, G. Fegan, S. D. Polley, L. Murungi, F. Verra, K. K. A. Tetteh, B. Lowe, T.

665 Mwangi, P. C. Bull, A. W. Thomas, D. R. Cavanagh, J. S. McBride, D. E. Lanar, M. J.

666 Mackinnon, D. J. Conway, K. Marsh, Breadth and magnitude of antibody responses to multiple

- 667 Plasmodium falciparum merozoite antigens are associated with protection from clinical malaria,
668 *Infection and Immunity* (2008), doi:10.1128/IAI.01585-07.
- 669 4. B. P. Gonçalves, C.-Y. Huang, R. Morrison, S. Holte, E. Kabyemela, D. R. Prevots, M. Fried,
670 P. E. Duffy, Parasite Burden and Severity of Malaria in Tanzanian Children, *New England*
671 *Journal of Medicine* **370**, 1799–1808 (2014).
- 672 5. W. Nahrendorf, A. Ivens, P. J. Spence, Inducible mechanisms of disease tolerance provide an
673 alternative strategy of acquired immunity to malaria, *eLife* **10** (2021), doi:10.7554/eLife.63838.
- 674 6. A. F. Cowman, J. Healer, D. Marapana, K. Marsh, Malaria: Biology and Disease *Cell* **167**,
675 610–624 (2016).
- 676 7. P. D. Crompton, J. Moebius, S. Portugal, M. Waisberg, G. Hart, L. S. Garver, L. H. Miller, C.
677 Barillas-Mury, S. K. Pierce, Malaria Immunity in Man and Mosquito: Insights into Unsolved
678 Mysteries of a Deadly Infectious Disease, *Annual Review of Immunology* **32**, 157–187 (2014).
- 679 8. C. Loiseau, M. M. Cooper, D. L. Doolan, Deciphering host immunity to malaria using systems
680 immunology, *Immunological Reviews* **293**, 115–143 (2020).
- 681 9. T. M. Tran, P. D. Crompton, Decoding the complexities of human malaria through systems
682 immunology *Immunological Reviews* **293**, 144–162 (2020).
- 683 10. M. M. Davis, C. M. Tato, D. Furman, Systems immunology: Just getting started *Nature*
684 *Immunology* **18**, 725–732 (2017).
- 685 11. T. M. Tran, R. Guha, S. Portugal, J. Skinner, A. Ongoiba, J. Bhardwaj, M. Jones, J. Moebius,
686 P. Venepally, S. Doumbo, E. A. DeRiso, S. Li, K. Vijayan, S. L. Anzick, G. T. Hart, E. M.
687 O’Connell, O. K. Doumbo, A. Kaushansky, G. Alter, P. L. Felgner, H. Lorenzi, K. Kayentao, B.
688 Traore, E. F. Kirkness, P. D. Crompton, A Molecular Signature in Blood Reveals a Role for p53
689 in Regulating Malaria-Induced Inflammation, *Immunity* (2019),
690 doi:10.1016/J.IMMUNI.2019.08.009.
- 691 12. S. E. Jong, V. Unen, M. D. Manurung, K. A. Stam, J. J. Goeman, S. P. Jochems, T. Hamp, N.
692 Pezzotti, Y. D. Mouwenda, M. Eunice Betouke Ongwe, F.-R. Lorenz, Y. C. M Kruize, S. Azimi,
693 M. H. Kamp, A. Vilanova, E. Eisemann, B. P. F Lelieveldt, M. Roestenberg, B. Kim Lee Sim,
694 M. J. T Reinders, R. Fendel, S. L. Hoffman, P. G. Kremsner, F. Koning, B. Mordmamp, B. Lell,
695 M. Yazdanbakhsh, Systems analysis and controlled malaria infection in Europeans and Africans
696 elucidate naturally acquired immunity, *Nature Immunology* (2021), doi:10.1038/s41590-021-
697 00911-7.

- 698 13. M. Vafa Homann, S. N. Emami, V. Yman, C. Stenström, K. Sondén, H. Ramström, M.
699 Karlsson, M. Asghar, A. Färnert, Detection of Malaria Parasites After Treatment in Travelers: A
700 12-months Longitudinal Study and Statistical Modelling Analysis, *EBioMedicine* **25**, 66–72
701 (2017).
- 702 14. M. Asghar, V. Yman, M. V. Homann, K. Sondén, U. Hammar, D. Hasselquist, A. Färnert,
703 Cellular aging dynamics after acute malaria infection: A 12-month longitudinal study, *Aging Cell*
704 (2018), doi:10.1111/accel.12702.
- 705 15. V. Yman, M. T. White, M. Asghar, C. Sundling, K. Sondén, S. J. Draper, F. H. A. A. Osier,
706 A. Färnert, Antibody responses to merozoite antigens after natural *Plasmodium falciparum*
707 infection: Kinetics and longevity in absence of re-exposure, *BMC Medicine* (2019),
708 doi:10.1186/s12916-019-1255-3.
- 709 16. C. Sundling, C. Rönnberg, V. Yman, M. Asghar, P. Jahnmatz, T. Lakshmikanth, Y. Chen, J.
710 Mikes, M. N. Forsell, K. Sondén, A. Achour, P. Brodin, K. E. M. Persson, A. Färnert, B cell
711 profiling in malaria reveals expansion and remodeling of CD11c⁺ B cell subsets, *JCI Insight*
712 (2019), doi:10.1172/jci.insight.126492.
- 713 17. E. Assarsson, M. Lundberg, G. Holmquist, J. Björkesten, S. Bucht Thorsen, D. Ekman, A.
714 Eriksson, E. Rennel Dickens, S. Ohlsson, G. Edfeldt, A.-C. Andersson, P. Lindstedt, J. Stenvang,
715 M. Gullberg, S. Fredriksson, J. D. Hoheisel, Ed. Homogenous 96-Plex PEA Immunoassay
716 Exhibiting High Sensitivity, Specificity, and Excellent Scalability, *PLoS ONE* **9**, e95192 (2014).
- 717 18. R. Argelaguet, B. Velten, D. Arnol, S. Dietrich, T. Zenz, J. C. Marioni, F. Buettner, W.
718 Huber, O. Stegle, Multi-Omics Factor Analysis—a framework for unsupervised integration of
719 multi-omics data sets, *Molecular Systems Biology* (2018), doi:10.15252/msb.20178124.
- 720 19. R. Argelaguet, D. Arnol, D. Bredikhin, Y. Deloro, B. Velten, J. C. Marioni, O. Stegle,
721 MOFA+: A statistical framework for comprehensive integration of multi-modal single-cell data,
722 *Genome Biology* **21**, 111 (2020).
- 723 20. B. Velten, J. M. Braunger, D. Arnol, R. Argelaguet, O. Stegle, Identifying temporal and
724 spatial patterns of variation from multi-modal data using MEFISTO, ,
725 doi:10.1101/2020.11.03.366674.
- 726 21. P. Jagannathan, F. Lutwama, M. J. Boyle, F. Nankya, L. A. Farrington, T. I. McIntyre, K.
727 Bowen, K. Naluwu, M. Nalubega, K. Musinguzi, E. Sikyomu, R. Budker, A. Katureebe, J. Rek,
728 B. Greenhouse, G. Dorsey, M. R. Kanya, M. E. Feeney, Vδ2⁺ T cell response to malaria

- 729 correlates with protection from infection but is attenuated with repeated exposure, *Scientific*
730 *Reports* **7**, 1–12 (2017).
- 731 22. L. A. Farrington, P. C. Callaway, H. M. Vance, K. Baskevitch, E. Lutz, L. Warriar, T. I.
732 McIntyre, R. Budker, P. Jagannathan, F. Nankya, K. Musinguzi, M. Nalubega, E. Sikyomu, K.
733 Naluwu, E. Arinaitwe, G. Dorsey, M. R. Kamya, M. E. Feeney, G. Hart, Ed. Opsonized antigen
734 activates V δ 2+ T cells via CD16/FC γ RIIIa in individuals with chronic malaria exposure, *PLOS*
735 *Pathogens* **16**, e1008997 (2020).
- 736 23. P. Jagannathan, C. C. Kim, B. Greenhouse, F. Nankya, K. Bowen, I. Eccles-James, M. K.
737 Muhindo, E. Arinaitwe, J. W. Tappero, M. R. Kamya, G. Dorsey, M. E. Feeney, Loss and
738 dysfunction of V δ 2+ γ δ T cells are associated with clinical tolerance to malaria, *Science*
739 *Translational Medicine* **6**, 251ra117-251ra117 (2014).
- 740 24. C. Junqueira, R. B. Polidoro, G. Castro, S. Absalon, Z. Liang, S. sen Santara, Â. Crespo, D.
741 B. Pereira, R. T. Gazzinelli, J. D. Dvorin, J. Lieberman, γ δ T cells suppress Plasmodium
742 falciparum blood-stage infection by direct killing and phagocytosis, *Nature Immunology* , 1–11
743 (2021).
- 744 25. L. A. Farrington, P. C. Callaway, H. M. Vance, K. Baskevitch, E. Lutz, L. Warriar, T. I.
745 McIntyre, R. Budker, P. Jagannathan, F. Nankya, K. Musinguzi, M. Nalubega, E. Sikyomu, K.
746 Naluwu, E. Arinaitwe, G. Dorsey, M. R. Kamya, M. E. Feeney, G. Hart, Ed. Opsonized antigen
747 activates V δ 2+ T cells via CD16/FC γ RIIIa in individuals with chronic malaria exposure, *PLOS*
748 *Pathogens* **16**, e1008997 (2020).
- 749 26. H. H. van Acker, A. Capsomidis, E. L. Smits, V. F. van Tendeloo, CD56 in the immune
750 system: More than a marker for cytotoxicity? *Frontiers in Immunology* **8**, 1 (2017).
- 751 27. W. Xu, A. Larbi, Heterogeneity in V δ 2pos T cell homeostasis in response to
752 stress *EBioMedicine* **43**, 31 (2019).
- 753 28. V. Appay, R. A. W. van Lier, F. Sallusto, M. Roederer, Phenotype and function of human T
754 lymphocyte subsets: Consensus and issues *Cytometry Part A* **73**, 975–983 (2008).
- 755 29. K. Deroost, J. Langhorne, Gamma/Delta T Cells and Their Role in Protection Against
756 Malaria, *Frontiers in Immunology* **9**, 2973 (2018).
- 757 30. H. Hsu, S. Boudova, G. Mvula, T. H. Divala, R. G. Mungwira, C. Harman, M. K. Laufer, C.
758 D. Pauza, C. Cairo, Prolonged PD1 Expression on Neonatal V δ 2 Lymphocytes Dampens

- 759 Proinflammatory Responses: Role of Epigenetic Regulation, *The Journal of Immunology* **197**,
760 1884–1892 (2016).
- 761 31. K. W. Dantzler, P. Jagannathan, $\gamma\delta$ T cells in antimalarial immunity: New insights into their
762 diverse functions in protection and tolerance *Frontiers in Immunology* (2018),
763 doi:10.3389/fimmu.2018.02445.
- 764 32. A. Ankan, I. M. N. Wortel, J. Textor, Testing Graphical Causal Models Using the R Package
765 “dagitty,” *Current Protocols* **1** (2021), doi:10.1002/cpz1.45.
- 766 33. T. W. Ademolue, Y. Aniweh, K. A. Kusi, G. A. Awandare, Patterns of inflammatory
767 responses and parasite tolerance vary with malaria transmission intensity, *Malaria Journal* **16**,
768 145 (2017).
- 769 34. T. M. Tran, M. B. Jones, A. Ongoiba, E. M. Bijker, R. Schats, P. Venepally, J. Skinner, S.
770 Doumbo, E. Quinten, L. G. Visser, E. Whalen, S. Presnell, E. M. O’connell, K. Kayentao, O. K.
771 Doumbo, D. Chaussabel, H. Lorenzi, T. B. Nutman, T. H. M. Ottenhoff, M. C. Haks, B. Traore,
772 E. F. Kirkness, R. W. Sauerwein, P. D. Crompton, Transcriptomic evidence for modulation of
773 host inflammatory responses during febrile *Plasmodium falciparum* malaria OPEN, (2016),
774 doi:10.1038/srep31291.
- 775 35. L. Farrington, H. Vance, J. Rek, M. Prah, P. Jagannathan, A. Katureebe, E. Arinaitwe, M. R.
776 Kanya, G. Dorsey, M. E. Feeney, Both inflammatory and regulatory cytokine responses to
777 malaria are blunted with increasing age in highly exposed children, *Malaria Journal* **16**, 499
778 (2017).
- 779 36. P. Jahnmatz, C. Sundling, V. Yman, L. Widman, M. Asghar, K. Sondén, C. Stenström, C.
780 Smedman, F. Ndungu, N. Ahlborg, A. Färnert, Memory B-Cell Responses Against Merozoite
781 Antigens After Acute *Plasmodium falciparum* Malaria, Assessed Over One Year Using a Novel
782 Multiplexed FluoroSpot Assay, *Frontiers in Immunology* **11**, 619398 (2021).
- 783 37. F. M. Ndungu, K. Lundblom, J. Rono, J. Illingworth, S. Eriksson, A. Färnert, Long-lived
784 *Plasmodium falciparum* specific memory B cells in naturally exposed Swedish travelers,
785 *European Journal of Immunology* (2013), doi:10.1002/eji.201343630.
- 786 38. A. Ortega-Pajares, S. J. Rogerson, The Rough Guide to Monocytes in Malaria
787 Infection *Frontiers in immunology* **9**, 2888 (2018).
- 788 39. S. P. Kurup, N. S. Butler, J. T. Harty, T cell-mediated immunity to malaria *Nature Reviews*
789 *Immunology* **19**, 457–471 (2019).

- 790 40. T. J. Suscovich, J. K. Fallon, J. Das, A. R. Demas, J. Crain, C. H. Linde, A. Michell, H.
791 Natarajan, C. Arevalo, T. Broge, T. Linnekin, V. Kulkarni, R. Lu, M. D. Slein, C. Luedemann,
792 M. Marquette, S. March, J. Weiner, S. Gregory, M. Coccia, Y. Flores-Garcia, F. Zavala, M. E.
793 Ackerman, E. Bergmann-Leitner, J. Hendriks, J. Sadoff, S. Dutta, D. A. Lauffenburger, E.
794 Jongert, U. Wille-Reece, G. Alter, *Mapping functional humoral correlates of protection against*
795 *malaria challenge following RTS,S/AS01 vaccination* (2020).
- 796 41. R. Guha, A. Mathioudaki, S. Doumbo, D. Doumtabe, J. Skinner, G. Arora, S. Siddiqui, S. Li,
797 K. Kayentao, A. Ongoiba, J. Zaugg, B. Traore, P. D. Crompton, J. W. Kazura, Ed. Plasmodium
798 falciparum malaria drives epigenetic reprogramming of human monocytes toward a regulatory
799 phenotype, *PLOS Pathogens* **17**, e1009430 (2021).
- 800 42. A. A. Patel, Y. Zhang, J. N. Fullerton, L. Boelen, A. Rongvaux, A. A. Maini, V. Bigley, R.
801 A. Flavell, D. W. Gilroy, B. Asquith, D. Macallan, S. Yona, The fate and lifespan of human
802 monocyte subsets in steady state and systemic inflammation, *Journal of Experimental Medicine*
803 **214**, 1913–1923 (2017).
- 804 43. P. A. Buffet, I. Safeukui, G. Deplaine, V. Brousse, V. Prendki, M. Thellier, G. D. Turner, O.
805 Mercereau-Puijalon, The pathogenesis of Plasmodium falciparum malaria in humans: Insights
806 from splenic physiology *Blood* **117**, 381–392 (2011).
- 807 44. S. Kho, L. Qotrunnada, L. Leonardo, B. Andries, P. A. I. Wardani, A. Fricot, B. Henry, D.
808 Hardy, N. I. Margyaningsih, D. Apriyanti, A. M. Puspitasari, P. Prayoga, L. Trianty, E.
809 Kenangalem, F. Chretien, I. Safeukui, H. A. del Portillo, C. Fernandez-Becerra, E. Meibalan, M.
810 Marti, R. N. Price, T. Woodberry, P. A. Ndour, B. M. Russell, T. W. Yeo, G. Minigo, R.
811 Noviyanti, J. R. Poespoprodjo, N. C. Siregar, P. A. Buffet, N. M. Anstey, Hidden Biomass of
812 Intact Malaria Parasites in the Human Spleen, *New England Journal of Medicine* **384**, 2067–
813 2069 (2021).
- 814 45. M. R. Mamedov, A. Scholzen, R. v. Nair, K. Cumnock, J. A. Kenkel, J. H. M. Oliveira, D. L.
815 Trujillo, N. Saligrama, Y. Zhang, F. Rubelt, D. S. Schneider, Y. hsiu Chien, R. W. Sauerwein,
816 M. M. Davis, A Macrophage Colony-Stimulating-Factor-Producing $\gamma\delta$ T Cell Subset Prevents
817 Malarial Parasitemic Recurrence, *Immunity* **48**, 350-363.e7 (2018).
- 818 46. A. Trampuz, M. Jereb, I. Muzlovic, R. M. Prabhu, Clinical review: Severe malaria *Critical*
819 *Care* **7**, 315–323 (2003).

- 820 47. J. Howard, I. Zaidi, S. Loizon, O. Mercereau-Puijalon, J. Déchanet-Merville, M. Mamani-
821 Matsuda, Human V γ 9V δ 2 T Lymphocytes in the Immune Response to *P. falciparum* Infection,
822 *Frontiers in Immunology* **9**, 2760 (2018).
- 823 48. D. I. Stanisic, J. Cutts, E. Eriksson, F. J. I. Fowkes, A. Rosanas-Urgell, P. Siba, M. Laman,
824 T. M. E. Davis, L. Manning, I. Mueller, L. Schofield, $\gamma\delta$ T cells and CD14⁺ Monocytes Are
825 Predominant Cellular Sources of Cytokines and Chemokines Associated With Severe Malaria,
826 *The Journal of Infectious Diseases* **210**, 295–305 (2014).
- 827 49. J. N. Che, O. P. G. Nmorsi, B. P. Nkot, C. Isaac, B. C. Okonkwo, Chemokines responses to
828 *Plasmodium falciparum* malaria and co-infections among rural Cameroonians, *Parasitology*
829 *International* **64**, 139–144 (2015).
- 830 50. M. N. Ajuebor, Y. Jin, G. L. Gremillion, R. M. Strieter, Q. Chen, P. A. Adegboyega, $\gamma\delta$ T
831 Cells Initiate Acute Inflammation and Injury in Adenovirus-Infected Liver via Cytokine-
832 Chemokine Cross Talk, *Journal of Virology* **82**, 9564–9576 (2008).
- 833 51. D. L. Hill, S. Innocentin, J. Wang, E. A. James, J. C. Lee, W. Kwok, M. Zand, E. J. Carr, M.
834 A. Linterman, Impaired HA-specific T follicular helper cell and antibody responses to, ,
835 doi:10.1101/2021.04.07.21255038.
- 836 52. V. Ryg-Cornejo, L. J. Ioannidis, A. Ly, C. Y. Chiu, J. Tellier, D. L. Hill, S. P. Preston, M.
837 Pellegrini, D. Yu, S. L. Nutt, A. Kallies, D. S. Hansen, Severe Malaria Infections Impair
838 Germinal Center Responses by Inhibiting T Follicular Helper Cell Differentiation, *Cell Reports*
839 **14**, 68–81 (2016).
- 840 53. K. Sondén, K. Wyss, I. Jovel, A. Vieira Da Silva, A. Pohanka, M. Asghar, M. V. Homann, L.
841 L. Gustafsson, U. Hellgren, A. Färnert, High Rate of Treatment Failures in Nonimmune
842 Travelers Treated With Artemether-Lumefantrine for Uncomplicated *Plasmodium falciparum*
843 Malaria in Sweden: Retrospective Comparative Analysis of Effectiveness and Case Series,
844 *Clinical Infectious Diseases Malaria Treatment Failures in Travelers • CID* **2017**, 199–206.
- 845 54. M. Asghar, V. Yman, M. V. Homann, K. Sondén, U. Hammar, D. Hasselquist, A. Färnert,
846 Cellular aging dynamics after acute malaria infection: A 12-month longitudinal study, *Aging Cell*
847 **17**, e12702 (2018).
- 848 55. H. Wickham, M. Averick, J. Bryan, W. Chang, L. D', A. McGowan, R. François, G.
849 Grolemond, A. Hayes, L. Henry, J. Hester, M. Kuhn, T. Lin Pedersen, E. Miller, S. M. Bache, K.
850 Müller, J. Ooms, D. Robinson, D. P. Seidel, V. Spinu, K. Takahashi, D. Vaughan, C. Wilke, K.

851 Woo, H. Yutani, RStudio 2 cynkra 3 Redbubble 4 Erasmus University Rotterdam 5 Flatiron
852 Health 6 Department of Integrative Biology, *Journal of Open Source Software* **4**, 1686 (2019).
853 56. Y. Benjamini, Y. Hochberg, Controlling the False Discovery Rate: A Practical and Powerful
854 Approach to Multiple Testing, *Journal of the Royal Statistical Society: Series B*
855 (*Methodological*) **57**, 289–300 (1995).
856 57. D. Makowski, M. Ben-Shachar, I. Patil, D. Lüdecke, Methods and Algorithms for
857 Correlation Analysis in R, *Journal of Open Source Software* **5**, 2306 (2020).
858 58. Z. Gu, L. Gu, R. Eils, M. Schlesner, B. Brors, Genome analysis circlize implements and
859 enhances circular visualization in R, **30**, 2811–2812 (2014).
860 59. Z. Gu, R. Eils, M. Schlesner, Complex heatmaps reveal patterns and correlations in
861 multidimensional genomic data, *Bioinformatics* (2016), doi:10.1093/bioinformatics/btw313.
862 60. FOR THE TREATMENT OF MALARIA GUIDELINES, (2015) (available at
863 www.who.int).
864
865
866
867

868 **Acknowledgments:**

869 We would firstly like to acknowledge the contribution of all the study participants. We would
870 also like to thank all involved clinicians, nurses especially Irene Nordling and Debbie Ribjer for
871 sampling and Fariba Foroogh for sample processing and organization. Further, we would like to
872 thank the team from the Translational Plasma Profile Facility at SciLifeLab for support and the
873 generation of data for this project. Figure 1A and 7G were created with BioRender.com.

874 **Funding:**

875 The Swedish Research Council grant 2019-01940 (CS)
876 Magnus Bergvall foundation grant 2017-02043 and 2018-02656 (CS)
877 Åke Wiberg foundation grant M18-0076 (CS)
878 Swedish Research Council 2015-02977, 2018-02688 and 2018-04468 (AF)
879 Region Stockholm 20150135 and 20180409 (AF)
880 Marianne and Marcus Wallenberg Foundation (AF)

881 **Author contributions:**

882 Conceptualization: CS, MJL, AF
883 Methodology: CS, MJL, NK, SA
884 Investigation: CS, MJL, KS, VY, NK, SA, DFP, AF
885 Visualization: CS, MJL
886 Funding acquisition: CS, AF
887 Project administration: CS
888 Supervision: CS, AF
889 Writing – original draft: CS, MJL
890 Writing – review & editing: CS, MJL, AF, KS, VY, NK, SA, DFP

891 **Competing interests:**

892 Authors declare that they have no competing interests.

893 **Data and materials availability:**

894 The flow cytometry data and plasma protein data (Olink Inflammation panel) generated during
895 this study are available upon request. Code used in the analyzes is available in repository:
896 <https://github.com/LautenbachMJ/MalariaTraveller>.